THE ASTROPHYSICAL JOURNAL SUPPLEMENT SERIES, 93:425–440, 1994 August

GALAXY PROPERTIES IN DIFFERENT ENVIRONMENTS. I. THE SAMPLE

MARCIO A. G. MAIA
Departamento de Astronomia, Observatório Nacional, Rua Gal. José Cristino 77, Rio de Janeiro 20921, RJ, Brazil
maia@on.br

AND

MIRIANI G. PASTORIZA, EDUARDO BICA, AND HORACIO DOTTORI
Departamento de Astronomia, Instituto de Física, Universidade Federal do Rio Grande do Sul, C.P. 15051, Porto Alegre 91501-970, RS, Brazil
Received 1993 September 1; accepted 1993 December 17

ABSTRACT

This paper presents two galaxy samples, respectively in a high and in a low local density environments, that were generated from the SSRS catalog using objective criteria. A preliminary comparison of physical properties in these two samples reveals that galaxies in high-density environments tend to be under a higher starbursting activity, have a deficiency of the neutral hydrogen content, present a higher fractional Seyfert population and a higher fraction of barred spirals as well. The present samples are intended to be used in future spectroscopic observations for more detailed investigation.

Subject headings: galaxies: clustering — galaxies: structure

1. INTRODUCTION

Evidence of several environmental effects have been reported to affect galaxy properties, for example, the well-studied morphology-density relation, which was first pointed out by Dressler (1980) for rich clusters, and revisited later by others (e.g., Postman & Geller 1984; Giovanelli, Haynes, & Chincarini 1986; Maia & da Costa 1990b). The effect consists of the fractional increase of early-type galaxies toward regions of high concentration of galaxies. Whitmore, Gilmore, & Jones (1993) claim that the morphology-clustercentric radius relation is more fundamental than the morphology-density one, after reexamining Dressler's (1980) sample of clusters. Nevertheless the impact of the local density of galaxies on the star formation rate (SFR) within those galaxies is not yet well understood. Two effects that influence the SFR in high-density regions are conceivable. On the one hand, the SFR could be enhanced by tidal interactions triggering star formation, possibly in the form of bursts (e.g., Bushouse 1986; Kennicutt et al. 1987). On the other hand, in the very high density regions in the cores of clusters, close galaxy encounters lead to a depletion of interstellar gas and thus leave preferentially anemic spirals in clusters of galaxies (Dressler 1984). In addition, for elliptical galaxies the evolution of mass-loss rate predicts the accumulation of gas in quantities far exceeding the observational upper limits. Much of this gas must have been removed from the galaxy. According to Gisler (1976) ablation of gas in galaxies by dense intercluster medium would be an efficient mechanism of gas removal. Galaxies located within superclusters are embedded in an environment with significantly higher density than the relatively isolated field galaxies within low-density regions, but close encounters are still not frequent enough to strip the gas from the galaxies in a way similar to that occurring within clusters (Maia & da Costa 1990b).

As a first approach the Hα equivalent width (EW) can be used to obtain information on the SFR in galaxies (Kennicutt & Kent 1983). Indeed Maia & da Costa (1990b) found that the Hα EW of galaxies within groups tends to be larger than in those outside groups. The Kolmogorov-Smirnov test significance level of the hypothesis that the distribution of the Hα EW in their high-density sample is different from that in their control sample is 97%. In terms of the above discussion, this could be interpreted as an enhanced star formation rate. However, the sample size was still subject to statistical fluctuations, and possible biases might have affected the sample generation. Moreover it is not yet clear the link between the Hα EW and the star formation rate (e.g., Kennicutt et al. 1987).

In this paper we present the selection procedure used to generate two samples of galaxies spanning all morphological types, respectively located in regions with an extremely high and low local densities of galaxies (§ 2). In § 3 we investigate physical properties of these galaxies as a function of the environment, such as the H I content, nuclear activity, presence of barred galaxies, and infrared luminosity. A summary is presented in § 4.

2. SAMPLE SELECTION

The Southern Sky Redshift Survey catalog (SSRS; da Costa et al. 1988, 1989, 1991) was taken as database for the sample selection. This catalog consists of 2028 galaxies, drawn from The ESO/Uppsala Survey of the ESO(B) Atlas (Lauberts 1982) satisfying the conditions:

$$\log [D(0)] \geq 0.1 ,$$

and

$$b^{II} \leq -30°, \quad \delta < -17\overset{\circ}{.}5 .$$

Here $D(0)$ is a "face-on" diameter defined by

$$\log [D(0)] = \log (D_1) - 0.235A(T) \log (R) ,$$

where

$$R = D_1/D_2$$

and $A(T)$ takes the values

$$A(T) = 0.950, \quad T < 0 ,$$
$$= 0.894, \quad T \geq 0 .$$

In these expressions D_1 is the major axis diameter, D_2 is the minor axis diameter, and T is the morphological type of the galaxies as listed by Lauberts (1982). Galaxies in binary and multiple systems, but listed in the ESO catalog as single entries, were examined, and those not fulfilling the diameter requirement were discarded from the SSRS sample. From the SSRS catalog, two subsamples were generated. One is formed by galaxies in a high-density environment (hereafter HDS), and the other named control sample (hereafter CS).

The HDS sample is formed by galaxies that are in groups of three or more members generated by the group finding algorithm described by Maia, da Costa, & Latham (1989). The groups are defined to be formed by the accumulation of galaxy pairs with a member in common, having projected separations D_{12} and line-of-sight velocity differences V_{12} satisfying

$$D_{12} = 2 \sin (\theta_{12}/2) V/H_o \leq D_L ,$$

$$V_{12} = |V_1 - V_2| \leq V_L ,$$

where $V = (V_1 + V_2)/2$, V_1 and V_2 are the radial velocities of the galaxies, θ_{12} their angular separation, and $H_o = 100$ km s^{-1} Mpc^{-1}. The search parameters D_L and V_L scale according to the expressions

$$D_L = D_0/[\phi(V)]^{1/3} ,$$

$$V_L = V_0/[\phi(V)]^{1/3} ,$$

where $D_0 = 0.136$ Mpc, and $V_0 = 400$ km s^{-1} are values of D_L and V_L chosen at a fiducial velocity $V_F = 1000$ km s^{-1}, and $\phi(V)$ is the selection function for the galaxy catalog being used, normalized by its value at V_F. The groups defined in such a way have a surrounding density contrast, $\delta\rho/\rho \geq 500$. This is equivalent to densities larger than 18.0 galaxies/Mpc^3. The procedure of weighting the search parameters by the selection function of the SSRS catalog assures a fixed number density enhancement relative to the mean.

The CS sample is made up of galaxies that turned out not to be assigned to any group in the procedure of search for neighbors as explained above. However, this search was performed at a $\delta\rho/\rho = 0.01$, which means that the selected objects are in regions of local densities smaller than 0.0004 galaxies/Mpc^3.

In Figure 1 we present the values of the search parameters D_L and V_L as a function of the distance for both samples. For the galaxies of HDS sample the values of D_{12} and V_{12} should be smaller than those represented by the curve. For CS galaxies, it means that there is no companion found with values of D_{12} and V_{12} below the line value for a given distance. All the selected objects have radial velocities (after correction for Virgo infall) smaller than 8000 km s^{-1}. This limit is smaller than that

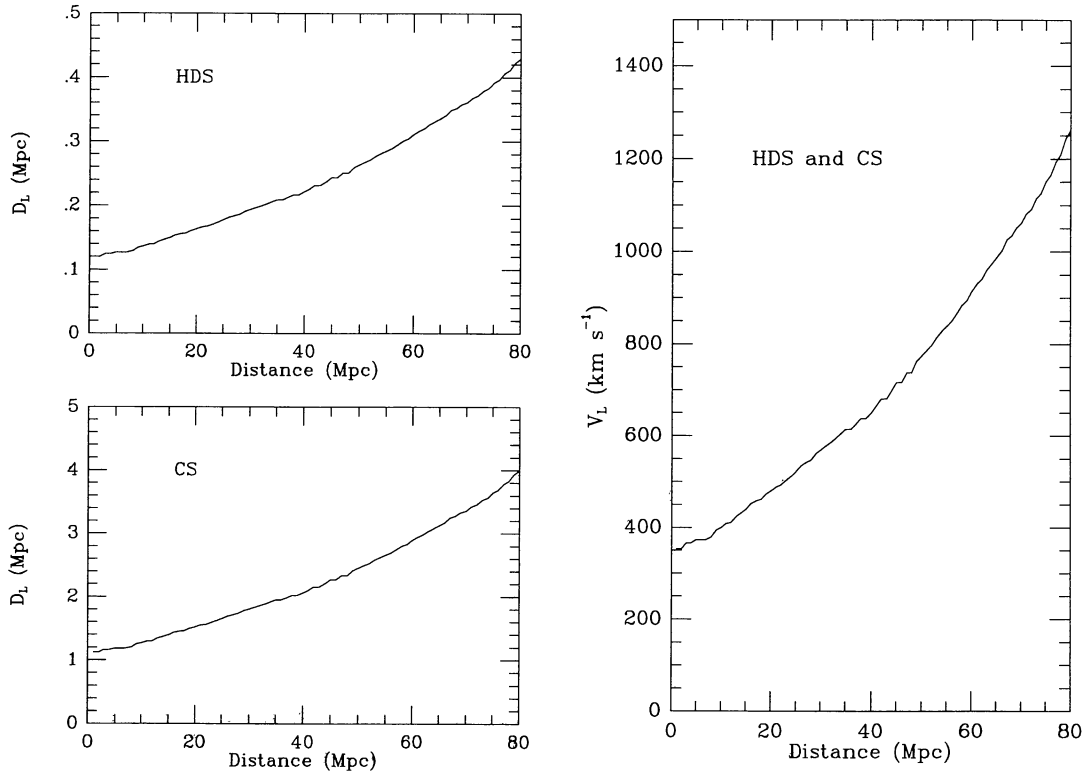

FIG. 1.—Search parameters D_L and V_L as a function of the radial velocity for HDS and CS samples

quoted by da Costa et al. (1988) of 9000 km s^{-1}, for which the sample can be considered statistically useful.

The derived HDS and CS samples contain, respectively, 151 and 179 galaxies, listed in Tables 1 and 2, which give the following information:

Column (1): The ESO-Uppsala identification number. The first three digits refer to ESO field number; the additional four digits are related to galaxy number, the last one used to indicate the existence of companions as described by Lauberts & Valentijn (1989).

Columns (2) and (3): The 1950.0 equatorial coordinates, taken from Lauberts (1982).

Column (4): Major and minor diameters, $a \times b$, in arcmin units as listed by Lauberts (1982).

Column (5): Total blue magnitude, B_T, taken from The Surface Photometry Catalog of the ESO-Uppsala Galaxies (Lauberts & Valentijn 1989).

Column (6): Absolute magnitude, M_B, calculated using $H_o = 100$ km s^{-1} Mpc^{-1}.

Column (7): Morphological type from Lauberts & Valentijn (1989).

Column (8): Heliocentric velocity, $V_\odot$, in km s^{-1}.

Some global characteristics of the selected objects for both samples can be examined in the plots of Figures 2 and 3. In Figure 2 we present the morphological type and velocity distributions. The effects of the morphological segregation can be clearly seen in the figure. There is an excess, as expected, of early-type galaxies in the HDS sample compared to the CS. Creating three subgroups of morphological types defined as early types (E to S0a), early spirals (Sa to Sc), and late spirals (S... to Irr), we find that the fractional population of these classes is 0.40/0.44/0.16 for HDS sample, whereas for the CS sample we derive 0.15/0.58/0.27. The results of the Kolmogorov-Smirnov test tell us that the probability that these two samples arise from the same parent distribution is smaller than 2.0×10^{-10}. In Figure 2 the frequency distribution of velocities for the HDS sample exhibits a pattern similar to that followed by groups of galaxies (see Fig. 1 of Maia & da Costa 1990a). In fact, the peak around $v \approx 1500$ km s^{-1} is due to member galaxies of groups such as Pavo, Grus, and Fornax (Maia et al. 1989). The velocity distribution for CS objects resembles that presented for all galaxies in the SSRS (Fig. 4*a* of da Costa et al. 1988), where the contribution of field galaxies is high. This behavior reinforces the confidence on the selection criteria used to generate the samples taking objects from two very different environments with respect to the galaxy number density. Distributions of apparent and absolute magnitudes from Tables 1 and 2 are presented in Figure 3. The more symmetrical distribution of the HDS in the absolute magnitude plot than that of the CS is related to excess of early-type galaxies in the HDS sample, which also populates the distribution tails with giant and dwarf ellipticals.

3. GALAXY PROPERTIES IN THE HDS AND CS SAMPLES

Using the information available in the literature, we conduct a preliminary analysis of several physical properties and characteristics of the galaxies from our two samples.

3.1. Hα *Emission Line*

Galaxy collisions and close encounters may play an important role in the star formation rate of galaxies, possibly triggering a starburst phase (e.g., Bushouse 1986; Kennicutt et al. 1987 and references therein; Moss & Whittle 1993). The Hα emission line could be used to measure the starburst activity of a galaxy (e.g., Kennicutt & Kent 1983). The spectra of spiral galaxies (types 1 to 6 from Tables 1 and 2) available in the SSRS database were examined to search for the Hα feature. The spatial region corresponds to the central zones of the galaxies, so we are probing eventual star formation events in the nuclear regions. Since the spectra were taken for redshift purposes, they were not flux calibrated, but they can be used to derive the equivalent width of the Hα emission line, whenever present. EW in Å and errors of its measurement for 11 galaxies of HDS sample and 29 for CS were obtained and are shown in Tables 3 and 4, respectively. A frequency distribution of EW is displayed in Figure 4. We do not have complete spectral information for all the galaxies in our samples, because there were redshifts available from the literature. Also, it is difficult to access what selection effects could be caused by this lack of completeness, but, if it exists, it should affect both samples equally. The sample sizes are not large, but in any case a Kolmogorov-Smirnov test tells us that the samples are different at a confidence level of 99%. The medians of the EW distributions are 40.3 and 10.1 Å for HDS and CS samples, respectively, reinforcing the idea of the link between emission properties and the frequency and strength of galaxy interactions. Of course, more detailed analysis is required, with the acquisition of flux-calibrated spectra of higher S/N for all galaxies in the present HDS and CS samples in order to improve the emission-line detection level.

3.2. H I *Content*

The amount of neutral hydrogen of a galaxy was found to be dependent on the environment for a same class of morphological type (e.g., Haynes & Giovanelli 1986; Magri et al. 1988; Huchtmeier & Richter 1989a; and more recently, Scodeggio & Gavazzi 1993). It was reported that galaxies in denser regions, such as the core of clusters of galaxies, are H I deficient. Ram pressure sweeping is normally the physical mechanism attributed to the H I removal.

We examine in this section the H I content for the spiral galaxies of our CS and HDS samples. No systematic observations have been carried out so far in order to get the 21 cm information. The parameters derived were obtained from the 21 cm data gathered throughout the literature, which are displayed in Tables 5 (44 galaxies) and 6 (52 galaxies) for CS and HDS samples, respectively, containing the following:

Column (1): The ESO-Uppsala name (as given in Tables 1 and 2).

Column (2): The morphological type (as described in Tables 1 and 2).

Column (3): Linear diameter D_B, in kiloparsecs, calculated using the major diameter of the ellipse at B surface brightness 25 mag/s arcsec^2 measured by Lauberts & Valentijn (1989) and the velocities quoted in Tables 1 and 2.

Column (4): 21 cm line flux corrected for galaxy self-absorp-

1994ApJS...93..425M

TABLE 1

OBJECTS IN HDS SAMPLE

ESO	Name	RA	Dec	a x b	B_T	M_B	Type	$V_\odot$	ESO	Name	RA	Dec	a x b	B_T	M_B	Type	$V_\odot$
151 0060	N 312	005403	−530312	1.5 x 1.3	13.4	-21.0	-4.0	7759	358 0260	I 335	033333	−343642	2.5 x 0.6	12.9	-17.6	-2.0	1284
151 0120		005435	−532206	1.6 x 0.9	13.9	-20.4	-1.7	7087	358 0270	N1379	033411	−353700	2.8 x 2.8	12.0	-18.0	-5.0	1003
151 0130	N 328	005444	−531136	3.4 x 0.6	14.3	-19.9	1.6	7005	548 0510	N1377	033426	−210359	2.3 x 1.0	13.4	-17.5	-2.0	1481
352 0460	N 491A	011746	−340948	2.3 x 1.0	14.3	-18.3	8.0	3260	358 0280	N1380	033430	−350800	5.0 x 2.8	11.0	-19.9	-3.0	1513
352 0470		011816	−342300	1.6 x 1.1	15.4	-17.3	10.0	3504	358 0290	N1381	033442	−352800	3.1 x 0.8	12.5	-18.2	-2.0	1403
352 0530	N 491	011906	−341900	1.5 x 1.1	13.3	-19.5	3.0	3577	358 0330	N1380A	033450	−345412	2.6 x 0.7	13.4	-17.1	-2.0	1250
353 0060	N 574	012647	−355124	1.4 x 1.0	14.2	-19.5	2.0	5445	358 0340		033450	−362512	2.0 x 1.8	13.8	-16.3	-1.0	1069
297 0060	N 626	013300	−392412	2.5 x 2.3	13.4	-20.2	5.5	5287	358 0350	N1386	033452	−360948	3.7 x 1.4	12.2	-16.6	-2.0	574
297 0080		013319	−393830	1.6 x 1.4	13.7	-19.8	1.5	5011	358 0360	N1387	033506	−354100	3.0 x 3.0	11.7	-18.2	-2.0	953
297 0090		013324	−393654	1.4 x 1.4	13.6	-20.2	-3.0	5629	358 0380	N1389	033518	−355500	2.6 x 1.6	12.4	-16.6	-2.0	637
153 0160		020307	−552700	2.0 x 1.0	15.1	-18.6	6.0	5442	548 0530	N1383	033522	−183006	2.0 x 0.8	13.4	-17.7	-2.0	1645
153 0170		020318	−552112	3.3 x 2.6	13.9	-20.1	5.0	6172	482 0170		033533	−230424	1.5 x 0.7	15.1	-15.2	2.0	1137
153 0200		020420	−552547	1.9 x 1.2	14.1	-19.6	3.0	5561	482 0180		033607	−233454	1.4 x 1.4	14.7	-16.0	-2.0	1368
545 0070	N 899	021935	−210200	1.8 x 1.4	13.1	-17.4	10.0	1259	482 0190	N1395	033619	−231125	5.0 x 4.5	10.7	-20.0	-5.0	1384
545 0100	N 907	022043	−205624	2.2 x 0.8	13.3	-17.5	5.0	1419	548 0580	N1393	033623	−183524	2.0 x 1.2	13.0	-18.4	-2.0	1882
545 0110	N 908	022046	−212742	5.8 x 2.8	11.0	-19.4	5.0	1202	358 0450	N1399	033634	−353642	4.0 x 4.0	9.7	-20.5	-4.0	1116
246 0180	I 1810	022731	−431747	1.5 x 1.4	14.2	-19.3	2.0	5073	482 0260	N1401	033711	−225311	2.8 x 0.8	13.3	-17.1	-2.0	1201
246 0210		022833	−431453	2.9 x 1.8	13.6	-20.0	3.0	5195	548 0650		033748	−193142	2.0 x 0.4	15.5	-14.3	-2.0	912
546 0140	N1098	024234	−175212	1.7 x 1.3	13.6	-20.7	5.0	7155	548 0660	I 343	033751	−183614	1.6 x 0.8	14.2	-16.8	-1.0	1566
546 0150	N1099	024258	−175505	2.3 x 0.8	14.0	-20.3	3.0	7314	548 0670	N1407	033756	−184422	2.5 x 2.5	10.6	-20.2	-4.3	1463
546 0180	N1100	024316	−175347	2.6 x 1.3	14.0	-20.3	1.0	7227	548 0680		033804	−190530	1.6 x 0.7	14.1	-16.8	-2.0	1513
416 0350		024826	−313605	1.4 x 1.2	14.5	-19.5	1.0	6322	548 0700	N1414	033845	−215224	1.9 x 0.4	14.7	-15.8	3.8	1241
357 0190	N1310	031909	−371647	2.2 x 1.7	13.0	-17.7	5.0	1408	482 0330	N1415	033846	−224325	3.6 x 2.1	12.5	-18.0	0.0	1248
357 0230	N1317	032047	−371700	3.4 x 2.5	11.8	-19.1	0.0	1546	548 0770	N1422	033919	−215024	3.0 x 0.7	14.0	-16.6	2.0	1306
357 0220	N1316	032047	−372306	8.5 x 7.5	9.2	-21.5	-2.0	1387	548 0780	I 346	033929	−182533	2.2 x 1.3	13.5	-17.5	-0.5	1595
548 0030	N1315	032053	−213311	1.8 x 1.7	13.5	-17.2	-2.0	1360	548 0790		033941	−190312	1.8 x 1.6	14.2	-17.0	1.0	1749
548 0070	N1325	032211	−214316	4.5 x 1.6	12.3	-18.2	3.5	1282	358 0520	N1427	034024	−353400	2.5 x 1.6	11.9	-18.2	-5.0	1047
548 0100	N1325A	032234	−213048	2.7 x 2.7	13.3	-16.7	7.0	1001	549 0020		034043	−191048	1.7 x 1.5	14.8	-14.8	10.0	829
548 0180	N1332	032403	−213030	4.0 x 1.7	11.4	-18.9	-3.0	1164	358 0540		034109	−362548	2.4 x 2.2	13.9	-14.8	8.0	545
548 0210		032522	−212406	3.0 x 0.6	14.6	-16.0	8.0	1344	358 0580	N1437	034143	−360042	3.5 x 2.4	12.5	-17.0	3.0	785
358 0090	N1351A	032651	−352100	3.0 x 0.6	14.2	-15.8	3.3	989	358 0610		034401	−363047	3.2 x 0.8	14.0	-16.3	10.0	1150
548 0290		032834	−211336	1.4 x 0.9	14.2	-15.8	3.0	1000	358 0620	N1460	034422	−365100	1.7 x 1.5	13.5	-16.5	-2.0	991
358 0120	N1351	032836	−350200	3.0 x 1.5	12.3	-18.1	-3.0	1179	358 0660		034600	−363730	1.8 x 0.8	15.6	-15.3	-3.5	1506
548 0310	N1353	032949	−205911	3.2 x 1.3	12.0	-18.5	3.0	1266	157 0050	N1536	040957	−563654	2.4 x 1.3	13.3	-16.6	5.0	936
548 0340		033044	−211523	1.4 x 1.4	14.3	-16.5	5.5	1451	157 0120	N1546	041329	−561100	3.7 x 2.0	12.3	-17.2	-1.0	790
358 0150		033110	−345830	1.6 x 0.9	15.3	-15.1	9.0	1204	157 0160	N1549	041438	−554254	3.6 x 2.8	10.5	-19.0	-5.0	793
548 0380	I 1953	033129	−213843	2.8 x 2.3	12.4	-18.5	6.0	1547	157 0170	N1553	041512	−555400	6.0 x 3.2	10.1	-19.7	-3.0	920
548 0390	N1359	033133	−193930	2.0 x 1.7	12.6	-18.5	9.0	1669	157 0180	I 2058	041650	−560318	3.3 x 0.5	13.9	-16.1	6.0	996
358 0170	N1365	033141	−361824	14.0 x 10.0	10.1	-20.5	3.0	1289	157 0260	N1581	042335	−550312	2.0 x 0.8	13.4	-17.1	-3.0	1241
548 0440		033204	−193524	1.5 x 0.7	14.3	-16.4	1.0	1390	157 0310	N1596	042629	−550800	4.4 x 1.0	12.0	-18.4	-2.0	1175
548 0470		033228	−191141	4.1 x 0.9	13.7	-16.9	-1.0	1301	157 0320	N1602	042648	−551000	2.4 x 1.2	13.8	-16.6	9.0	1180
358 0210	N1373	033302	−352012	1.4 x 1.0	14.0	-16.1	-3.0	1037	118 0430	N1672	044454	−592000	9.0 x 8.0	10.5	-19.5	4.0	989
548 0490		033315	−212253	1.6 x 0.8	15.4	-15.0	7.0	1198	119 0060	N1688	044742	−595300	3.0 x 2.3	12.6	-17.1	7.5	876
358 0240	N1375	033318	−352553	2.2 x 0.8	13.0	-15.1	-3.0	409	119 0190	N1703	045207	−594930	4.5 x 4.5	12.3	-18.0	5.0	1156
358 0230	N1374	033323	−352400	2.3 x 2.0	12.0	-18.0	-3.0	1004	305 0060	N1792	050330	−380300	8.0 x 4.0	10.7	-19.0	3.4	876
548 0500	I 1962	033325	−212723	3.8 x 0.9	14.7	-16.1	8.0	1475	305 0080	N1808	050559	−373400	10.0 x 7.0	10.8	-18.2	1.0	643

TABLE 1—*Continued*

ESO	Name	RA	Dec	a x b	B_T	M_B	Type	$V_\odot$
362 0060	N1827	050823	−370200	3.5 x 0.7	13.3	-16.0	6.0	717
119 0540		051946	−611830	1.5 x 0.8	14.3	-19.1	0.0	4812
119 0550		051948	−612042	2.5 x 1.0	13.7	-19.5	1.0	4439
119 0580		052041	−610624	1.6 x 0.6	14.5	-18.9	0.0	4832
233 0320	N6861	200341	−483100	2.5 x 1.4	12.0	-20.1	-5.0	2652
233 0340	N6861D	200442	−482100	2.3 x 0.8	13.5	-18.3	-3.0	2326
233 0390	N6868	200619	−483123	3.0 x 2.2	11.6	-20.6	-5.0	2708
233 0410	N6870	200636	−482600	2.9 x 1.5	13.2	-18.7	2.0	2442
284 0290	N6878A	201005	−445805	2.2 x 1.0	14.0	-19.6	4.0	5173
284 0320		201023	−443012	1.4 x 1.4	13.7	-20.0	0.0	5581
284 0310	N6878	201023	−444042	2.0 x 1.5	13.7	-20.1	4.0	5659
284 0330		201042	−444630	1.5 x 0.7	14.2	-19.6	-2.0	5694
234 0130		201850	−505447	1.6 x 0.6	14.7	-18.6	4.0	4654
285 0050	N6902B	201941	−440154	1.8 x 1.8	14.2	-18.0	5.0	2817
234 0160		201945	−504224	1.5 x 1.2	14.6	-18.9	5.0	5011
285 0070		202036	−440930	2.8 x 1.2	12.8	-19.4	-0.7	2743
234 0220	N6899	202042	−503542	1.8 x 1.1	13.5	-20.2	4.0	5535
285 0080	N6902	202102	−434856	9.0 x 6.0	11.8	-20.3	4.0	2623
235 0490		210115	−482317	1.6 x 1.0	13.7	-19.6	-5.0	4610
235 0550		210229	−482423	3.5 x 3.5	13.0	-20.4	5.0	4820
235 0570		210256	−482212	2.7 x 0.7	14.2	-19.3	4.0	4953
286 0820		211231	−423805	1.5 x 1.1	14.5	-18.9	5.0	4712
288 0260	N7162	215633	−433248	3.7 x 1.4	13.4	-18.2	5.0	2063
288 0270	N7166	215727	−433747	2.6 x 1.1	12.6	-19.2	-3.0	2242
288 0280	N7162A	215730	−432254	3.9 x 3.0	13.5	-18.1	9.0	2052
466 0360		215826	−314612	1.8 x 0.6	14.3	-17.4	1.0	2210
466 0380	N7172	215906	−320627	2.5 x 1.3	12.8	-19.1	1.0	2391
466 0390	N7173	215909	−321300	1.5 x 1.0	12.1	-19.9	-3.5	2511
466 0400	N7174	215912	−321352	1.8 x 0.8	12.3	-19.8	-0.5	2593
466 0460		215948	−321353	1.6 x 0.6	14.8	-16.8	-2.0	2115
404 0270		220053	−323136	3.5 x 1.5	13.4	-18.5	4.7	2359
108 0110	N7179	220106	−641717	2.1 x 1.0	13.4	-18.7	3.3	2669
108 0130	N7191	220310	−645242	1.6 x 0.6	13.8	-18.3	3.5	2658
467 0070	N7203	220345	−312430	2.1 x 1.1	13.6	-18.2	0.0	2305
467 0081	N7204N	220400	−311742	2.0 x 1.1	14.5	-17.4	3.0	2405
467 0082	N7204S	220400	−311818	2.0 x 1.1	14.9	-17.0	3.5	2405
289 0080	N7233	221233	−460548	1.8 x 1.6	12.9	-18.1	1.0	1599
289 0070	N7232	221233	−460600	3.0 x 1.0	12.6	-18.5	9.0	1645
289 0090	N7232B	221248	−465600	2.0 x 1.8	13.5	-17.8	9.0	1800
109 0180	N7358	224215	−652300	2.0 x 0.6	13.6	-18.8	-2.0	3053
109 0221	I 5250E	224400	−651918	1.3 x 1.2	12.1	-20.2	-2.0	2920
109 0220	I 5250W	224412	−651900	3.5 x 3.5	13.6	-18.7	-3.0	2829
290 0260	I 5267A	225304	−434205	3.0 x 1.0	13.8	-16.7	4.0	1246
406 0260	I 5269B	225348	−363000	5.5 x 1.1	13.5	-17.3	6.0	1417
406 0250	N7418	225348	−371748	4.6 x 3.2	11.7	-18.7	5.0	1200
406 0270	N7418A	225353	−370100	3.6 x 2.0	13.9	-17.4	7.0	1806
290 0270	I 5267B	225404	−440142	1.7 x 0.7	13.4	-17.4	-2.0	1436
406 0290	I 5264	225405	−364900	2.7 x 0.6	13.5	-17.8	1.8	1800
346 0170	N7421	225405	−373700	2.2 x 2.0	12.6	-18.4	4.5	1586
406 0300	I 1459	225421	−364347	5.0 x 3.5	10.9	-19.8	-5.0	1381
290 0290	I 5267	225422	−433952	8.0 x 5.0	11.2	-19.6	1.0	1456
406 0330	I 5270	225505	−360730	4.0 x 0.9	13.0	-18.0	6.0	1616
291 0120	N7552	231324	−425200	4.5 x 4.0	11.2	-19.4	2.5	1316
291 0160	N7582	231536	−423835	8.0 x 3.0	10.9	-19.7	1.0	1304
347 0330	N7590	231612	−423100	2.9 x 1.2	12.1	-18.4	3.0	1235
347 0340	N7599	231635	−423200	5.0 x 1.6	11.9	-18.9	3.0	1418
240 0100		233503	−474654	3.0 x 1.6	12.5	-19.8	-2.0	2885
240 0110		233506	−480012	7.0 x 0.7	13.1	-18.9	4.8	2521
240 0130		233645	−480300	1.6 x 1.1	14.1	-18.2	3.0	2938

1994ApJS...93..425M

TABLE 2

OBJECTS IN CS SAMPLE

ESO	Name	RA	Dec	a x b	B_T	M_B	Type	$V_\odot$	ESO	Name	RA	Dec	a x b	B_T	M_B	Type	$V_\odot$
409 0220	N 7	000548	−301145	2.7 x 0.6	13.9	-16.6	6.0	1246	477 0180	N 775	015615	−263205	1.9 x 1.5	13.4	-19.7	4.0	4238
241 0210		000749	−464147	2.7 x 0.6	14.3	-19.5	4.0	5812	013 0280		020305	−795400	2.4 x 0.4	15.3	-17.8	4.0	4256
050 0060		001136	−701800	2.0 x 2.0	14.5	-18.4	6.0	3813	478 0020	N 823	020503	−254047	1.5 x 1.4	13.6	-19.5	3.5	4116
111 0200	N 53	001215	−603624	2.5 x 1.7	13.7	-19.4	3.0	4243	478 0060		020700	−233905	2.2 x 1.2	13.2	-20.3	4.0	5012
539 0050		001437	−193442	1.9 x 1.2	13.5	-18.8	5.0	2949	298 0140		020824	−421923	1.9 x 0.9	15.5	-17.4	10.0	3815
194 0120	N 92	001904	−485412	3.2 x 1.2	13.7	-18.7	1.0	2987	030 0080		020851	−761030	2.7 x 0.5	14.9	-14.9	7.0	930
150 0050		002001	−535524	4.3 x 2.8	14.0	-16.2	8.0	1105	355 0070	N 897	021857	−335700	2.2 x 1.5	13.1	-20.1	1.0	4418
242 0050	N 98	002022	−453247	1.8 x 1.4	13.6	-20.2	5.0	5858	478 0280	N 922	022249	−250056	1.9 x 1.7	12.5	-19.7	9.0	2769
350 0140	N 101	002123	−324847	2.8 x 2.8	13.4	-19.1	6.0	3111	545 0210	N 947	022613	−191348	2.8 x 1.5	13.4	-20.0	5.0	4712
350 0270		002835	−370953	1.4 x 0.9	15.1	-19.1	3.0	6994	479 0080	N 951	022640	−223424	1.5 x 0.8	15.5	-18.3	2.0	5839
079 0020		002946	−644000	2.3 x 0.3	14.6	-17.3	7.1	2426	198 0130		022726	−484247	2.5 x 1.8	13.7	-19.8	2.0	5093
242 0140		003200	−435600	1.6 x 1.2	14.2	-19.6	-2.0	5628	355 0260		023012	−351500	1.9 x 1.0	13.8	-17.3	4.0	1674
411 0010	N 174	003430	−294500	1.8 x 0.7	13.8	-18.7	0.0	3182	355 0300		023530	−330830	2.5 x 1.2	13.6	-19.5	4.0	4230
474 0050	N 172	003445	−225135	2.5 x 0.4	14.7	-17.4	3.8	2662	479 0200		023652	−225235	2.6 x 0.7	14.9	-17.3	4.6	2730
540 0070	N 179	003516	−180730	1.4 x 1.0	14.0	-19.8	-3.0	5778	416 0070	I 1833	023928	−282306	1.9 x 1.1	14.1	-19.2	-1.0	4607
242 0230		003652	−432100	1.8 x 0.7	13.9	-18.9	5.0	3715	115 0280	N1096	024231	−600724	2.2 x 2.2	13.7	-20.2	4.0	6106
295 0010		004009	−423053	1.6 x 1.6	16.0	-17.7	7.0	5461	416 0250		024634	−314435	2.4 x 0.4	14.7	-18.6	3.0	4653
411 0100		004326	−312817	1.8 x 1.4	14.7	-19.0	4.0	5536	417 0080	N1165	025642	−321747	3.8 x 1.3	13.7	-19.6	0.5	4552
351 0050		004418	−360411	1.5 x 1.2	15.2	-18.6	6.0	5816	031 0050		025824	−743917	2.8 x 1.2	14.1	-19.1	3.5	4466
540 0210		004428	−220711	1.4 x 0.9	15.0	-19.0	3.0	6295	546 0370		025828	−222017	1.8 x 1.0	14.8	-18.2	8.0	4052
295 0100		004732	−395435	1.7 x 0.6	14.2	-20.0	1.0	6937	481 0070		030958	−251906	1.8 x 1.8	14.3	-19.6	0.0	6161
079 0070		005024	−652953	2.2 x 0.5	13.7	-20.3	8.0	6242	357 0130	N1288	031512	−324538	2.5 x 2.5	12.8	-20.3	5.0	4183
112 0100	I 1597	005122	−582247	2.1 x 0.4	15.0	-18.4	3.0	4715	301 0140		032325	−400418	1.6 x 1.5	15.0	-18.0	7.0	3926
351 0180		005125	−333400	1.6 x 0.6	15.2	-18.4	4.0	5143	482 0010		032912	−264400	2.0 x 0.5	14.8	-18.2	3.0	4045
541 0010		005235	−191636	2.4 x 1.5	14.0	-19.9	3.5	6042	482 0020		032948	−251036	1.7 x 1.0	14.8	-19.2	3.0	6208
295 0250	N 324	005455	−411341	1.7 x 0.5	14.1	-18.4	-2.0	3127	083 0060		033110	−624417	2.4 x 1.0	15.0	-18.5	4.3	5072
051 0110		005808	−682347	2.0 x 2.0	14.1	-20.0	3.0	6610	548 0750		033907	−175500	1.8 x 1.8	14.0	-20.2	5.0	6866
151 0190		010011	−543542	2.0 x 1.5	14.9	-15.2	9.0	1046	419 0030		034006	−280130	1.9 x 1.2	13.6	-19.3	4.0	3847
013 0120		010621	−803424	3.4 x 0.8	13.5	-19.5	-3.0	3935	031 0200		034241	−771736	1.8 x 1.1	14.9	-18.4	4.3	4505
080 0010		011205	−623954	1.6 x 0.8	14.9	-18.4	6.0	4566	482 0430	N1459	034450	−254035	2.4 x 1.6	13.6	-19.3	4.0	3885
475 0140		011310	−264247	2.7 x 0.5	14.6	-18.1	9.0	3473	083 0100		034503	−642717	2.0 x 1.1	15.0	-18.6	6.0	5190
542 0040		011705	−210217	1.6 x 1.2	15.0	-18.6	8.0	5208	302 0070		034514	−373153	2.0 x 1.4	15.0	-18.7	5.0	5400
296 0130	N 482	011806	−411336	2.5 x 0.6	14.5	-19.5	0.0	6234	549 0220		034636	−190748	2.0 x 0.9	14.9	-18.1	5.0	3991
476 0040		011845	−265917	2.4 x 0.8	13.9	-19.8	-2.9	5551	419 0120		035508	−290112	2.0 x 0.3	14.2	-18.7	1.0	3782
196 0100		012841	−512353	1.9 x 0.8	14.5	-18.1	6.0	3291	483 0060		035820	−251917	3.5 x 0.6	14.1	-18.8	3.0	3832
296 0380		013015	−385612	1.3 x 1.3	14.0	-18.6	4.0	3347	550 0050		040345	−175435	3.0 x 0.9	14.7	-16.3	8.5	1593
476 0270		013253	−225735	1.6 x 0.8	15.7	-18.0	7.5	5391	420 0030		040546	−295930	2.5 x 1.7	13.5	-19.4	5.0	3774
114 0010		013556	−610705	1.7 x 0.8	14.8	-18.7	5.6	5077	201 0220		040734	−485124	2.9 x 0.4	14.7	-18.1	5.0	3678
244 0440		013649	−470524	2.0 x 1.0	14.2	-19.8	1.0	6370	420 0080		040851	−300317	1.5 x 1.1	14.4	-19.2	4.0	5285
029 0530	N 643B	013825	−751500	1.8 x 0.4	14.6	-18.2	-2.0	3637	420 0170		041830	−315035	1.8 x 0.5	13.9	-18.1	-2.0	2468
543 0120		014018	−182847	1.7 x 0.8	...	...	3.0	4715	202 0140	N1578	042228	−514247	1.4 x 1.2	13.8	-20.0	1.0	5819
080 0060		014544	−631311	1.4 x 1.0	14.4	-15.9	8.7	1150	118 0230	I 2070	042339	−580535	1.8 x 1.2	14.5	-19.6	5.0	6688
152 0240	N 685	014548	−530100	5.0 x 4.5	12.0	-18.0	6.0	981	084 0180		042710	−624205	1.3 x 1.3	14.0	-19.6	0.5	5346
477 0060	N 686	014636	−240247	1.5 x 1.3	13.4	-19.8	-3.0	4311	484 0250	N1591	042728	−264917	1.5 x 1.0	13.8	-19.1	2.0	3806
354 0180	I 1759	015543	−331348	2.2 x 2.2	13.8	-18.9	5.0	3521	551 0130		043110	−184654	1.8 x 1.0	14.5	-19.4	6.0	6078
297 0370		015606	−394717	2.4 x 0.5	14.6	-19.0	4.7	5156	084 0260		043601	−651430	2.3 x 0.5	14.2	-19.3	-1.0	5118

TABLE 2—*Continued*

ESO	Name	RA	Dec	a x b	B_T	M_B	Type	$V_\odot$
485 0060		043809	−242453	1.4 x 1.2	14.5	-18.6	6.0	4111
551 0300		044013	−173254	2.1 x 1.5	14.9	-18.1	7.0	3903
304 0160	N1658	044222	−413317	1.8 x 0.6	14.4	-19.0	4.0	4862
203 0020		044548	−500818	1.5 x 1.0	14.8	-18.7	6.0	5065
485 0120		044559	−251900	2.2 x 0.4	15.0	-18.1	5.0	4226
304 0260		044925	−395635	1.5 x 1.0	15.2	-18.6	1.0	5878
361 0190		045307	−372400	2.3 x 0.8	14.2	-17.3	1.0	2027
422 0120	I 2106	045435	−283447	2.2 x 1.2	13.8	-19.5	4.0	4638
422 0270		050314	−315105	1.8 x 1.1	14.2	-18.8	5.0	3957
203 0180	N1803	050408	−493800	1.5 x 0.9	13.5	-19.3	4.0	3711
305 0140		051055	−395505	1.7 x 1.0	14.1	-19.2	5.0	4540
486 0400		051333	−224547	1.5 x 0.7	14.8	-18.9	3.0	5486
362 0140	I 2122	051716	−370818	1.3 x 1.2	13.8	-19.4	-2.5	4319
016 0020	N1956	052206	−774642	2.5 x 1.1	14.1	-19.2	0.6	4522
253 0040	N1930	052429	−464617	2.0 x 1.4	13.4	-19.5	-5.0	3883
204 0190	N2007	053347	−505712	2.0 x 0.7	14.8	-18.3	6.0	4214
159 0230		053913	−553347	1.8 x 0.9	14.4	-19.8	3.0	6842
160 0020		055011	−533500	2.1 x 0.5	13.9	-19.2	2.5	4212
142 0500	I 4901	195012	−585042	6.0 x 4.0	12.3	-19.1	5.0	1920
233 0130	I 4916	195435	−502423	1.5 x 1.5	14.4	-19.0	3.0	4771
105 0200		195808	−641306	2.1 x 0.2	16.1	-17.5	6.0	5346
339 0320	N6849	200253	−402030	1.5 x 1.0	12.9	-21.0	-5.0	5924
462 0150		202011	−275212	2.2 x 1.7	12.9	-20.9	-5.0	5703
340 0420		203137	−404747	1.9 x 1.7	14.5	-17.5	8.0	2468
528 0340		203932	−241953	2.2 x 1.2	14.7	-19.1	5.0	5711
106 0120	I 5038	204228	−651200	1.6 x 0.8	14.2	-18.8	6.0	3916
341 0150	N6958	204523	−381053	2.5 x 2.0	12.3	-19.7	-3.0	2476
074 0190	I 5054	204848	−711248	2.1 x 0.4	14.0	-19.0	1.0	4008
342 0010		210113	−400530	1.6 x 0.8	14.9	-19.2	5.5	6741
187 0480	N7007	210153	−524500	2.3 x 1.5	12.9	-19.3	-3.0	2736
286 0500		210324	−424524	1.6 x 0.8	13.8	-18.1	-3.0	2452
464 0250		210532	−295817	1.7 x 1.7	13.7	-20.1	-3.0	5822
107 0160		211159	−650130	3.2 x 0.4	15.2	-15.8	8.0	1602
235 0840		211430	−483647	1.6 x 1.4	14.7	-19.4	7.7	6658
342 0350		211658	−395847	2.0 x 2.0	13.8	-19.0	1.0	3578
145 0050	N7059	212336	−601400	4.4 x 2.1	12.5	-17.9	7.0	1190
530 0510		212452	−235312	1.3 x 1.3	17.4	-13.7	7.0	1682
287 0460		213649	−441917	1.9 x 1.2	14.3	-19.0	6.0	4578
403 0120		213650	−361548	1.7 x 1.6	13.8	-19.7	1.0	4943
600 0070		213904	−174024	1.5 x 1.5	...	...	6.0	5813
188 0170	N7106	213912	−525542	2.9 x 1.6	13.8	-18.6	4.8	3039
466 0050		214237	−291817	1.6 x 0.9	15.2	-18.6	3.0	5767
343 0280		214420	−385642	1.9 x 0.5	15.7	-17.5	4.0	4413
237 0020	N7124	214448	−504800	3.7 x 1.4	13.3	-20.2	4.5	4939
466 0110	I 5139	214729	−311341	2.6 x 1.2	13.3	-20.3	-3.0	5191
189 0070	N7141	214848	−554817	6.0 x 4.0	12.7	-19.5	4.0	2725
145 0220	I 5141	214942	−594400	1.8 x 1.4	13.5	-19.6	4.5	4212
075 0370	I 5140	215017	−673400	2.4 x 0.3	15.2	-17.6	6.5	3695
404 0110		215345	−364347	2.0 x 1.1	14.9	-18.8	3.0	5598
532 0090	N7167	215741	−245224	2.0 x 1.8	13.2	-18.7	5.0	2422
601 0040		215843	−221842	2.3 x 0.7	14.6	-18.9	4.6	5009
237 0270	I 5152	215926	−513217	6.0 x 4.0	11.0	-9.0	10.0	10
237 0300		215950	−504100	1.5 x 0.8	14.7	-18.9	3.0	5140
601 0120		220105	−200724	2.2 x 0.6	14.4	-19.2	3.0	5236
601 0190		220441	−210518	2.0 x 0.7	15.0	-19.2	6.0	7030
146 0090	N7205	220506	−574000	4.0 x 2.1	11.8	-18.9	5.0	1403
532 0220		220621	−272447	1.7 x 0.8	14.7	-16.9	5.4	2087
146 0140		220929	−621853	3.2 x 0.2	15.2	-15.6	7.0	1461
108 0200	I 5176	221111	−670548	4.8 x 0.7	13.5	-17.3	3.9	1445
533 0060		221316	−265547	1.6 x 0.7	14.4	-19.8	3.0	6930
289 0180	I 5201	221754	−461700	11.0 x 6.0	11.5	-17.6	8.0	669
146 0200	I 5203	221913	−600136	1.4 x 0.9	14.7	-18.6	5.0	4473
146 0220	I 5207	222006	−604905	1.4 x 0.9	15.2	-18.9	6.0	6540
467 0490	N7258	222009	−283554	1.8 x 0.8	13.9	-18.9	3.0	3687
405 0180	N7267	222130	−335647	1.8 x 1.5	13.0	-19.5	1.0	3137
533 0450		222944	−255512	2.6 x 2.4	13.4	-20.3	3.0	5580
602 0270		223018	−202100	1.6 x 1.6	14.4	-19.3	6.0	5543
533 0480		223148	−225705	1.6 x 0.6	14.7	-19.0	3.0	5477
534 0110	N7341	223622	−225535	3.1 x 1.3	13.3	-19.8	1.3	4191
238 0240		224145	−493230	1.5 x 0.7	...	...	3.0	6758
109 0210	I 5249	224347	−650541	4.4 x 0.5	14.4	-17.1	7.0	2038
534 0310		225258	−241318	1.7 x 1.0	14.6	-19.2	6.0	5851
290 0350		225839	−465454	2.5 x 0.4	15.1	-18.6	4.7	5570
290 0450	N7476	230216	−432212	1.5 x 1.2	13.6	-18.5	2.0	2685
407 0130		231321	−360800	1.4 x 1.2	15.1	-17.8	6.0	3859
407 0140		231453	−350354	2.4 x 1.6	13.5	-18.5	5.0	2504
535 0150		231624	−225924	2.9 x 1.4	...	...	6.0	5839
605 0070	I 5321	232343	−181348	1.6 x 1.0	14.0	-18.1	3.0	2676
292 0140		233956	−451053	3.0 x 0.5	14.0	-16.5	5.0	1283
292 0170	N7744	234224	−431200	3.0 x 2.4	12.5	-19.7	-2.0	2807
149 0010		234512	−572100	5.0 x 1.0	13.6	-17.1	7.8	1410
471 0200	N7755	234515	−304751	3.8 x 2.6	12.1	-20.1	4.5	2708
606 0110		234625	−195812	1.7 x 1.2	14.7	-19.0	5.0	5564
472 0100		235240	−240641	1.8 x 0.8	14.7	-18.2	4.5	3735
193 0060		235358	−484212	1.6 x 1.4	14.6	-18.0	5.0	3387
012 0120		235747	−810411	1.6 x 1.5	13.9	-20.5	4.0	7594
293 0270		235754	−404542	2.8 x 0.7	14.4	-17.9	4.0	2863

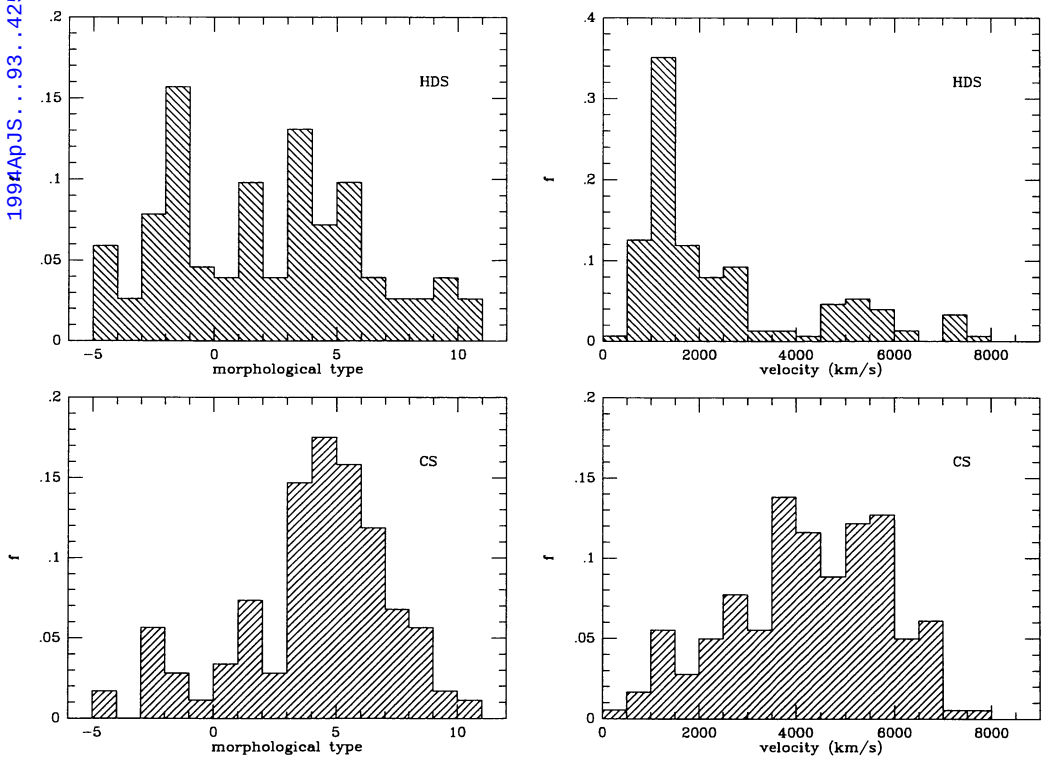

FIG. 2.—Morphological type and velocity distributions for galaxies of HDS and CS samples

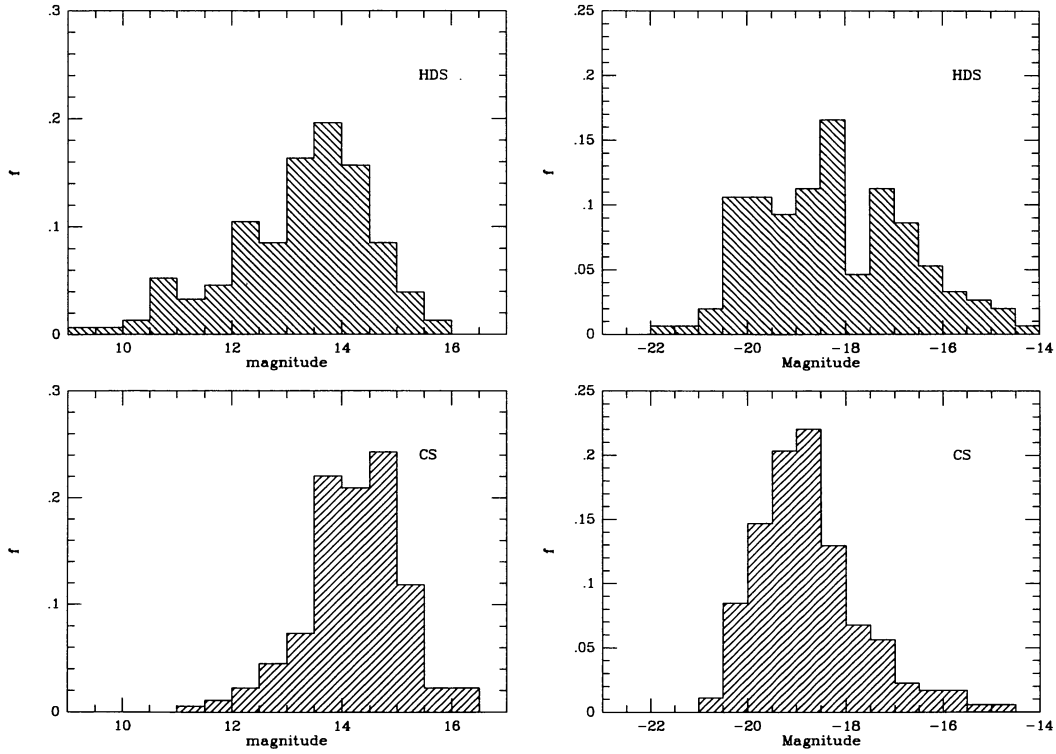

FIG. 3.—Apparent and absolute magnitude distributions for galaxies of Tables 1 and 2

TABLE 3

Hα EW FOR OBJECTS IN HDS SAMPLE

ESO	Hα EW	RMS
352 0530	2.5	0.6
353 0060	66.2	3.1
546 0150	9.9	0.6
358 0170	40.4	0.8
118 0430	27.1	0.3
305 0080	57.1	1.0
234 0130	32.0	1.5
466 0360	11.1	0.7
406 0330	41.1	3.4
291 0120	47.3	1.0
291 0160	68.7	1.2

tion (F_c) in Jy/km s^{-1} as described by Haynes & Giovanelli (1984).

Column (5): The logarithm of the neutral hydrogen mass $M_{\rm H\,I}$, in solar masses ($M_\odot$) given by

$$M_{\rm H\,I} = 2.356 \times 10^5 d^2 F_c ,$$

where d is the distance in Mpc (H_o = 100 km s^{-1} Mpc^{-1}).

Column (6): *Pseudo* H I surface density $\sigma_{\rm H\,I}$, in $M_\odot$ pc^{-2}, which is the total H I mass divided by the optical area of the galaxy, stated by

$$\sigma_{\rm H\,I} = M_{\rm H\,I}/(\pi/4)D_B^2) .$$

TABLE 4

Hα EW FOR OBJECTS IN CS SAMPLE

ESO	Hα EW	RMS
409 0220	19.2	1.4
194 0120	117.9	2.2
350 0140	8.5	0.9
351 0180	20.9	2.6
051 0110	27.8	0.8
543 0120	6.1	0.8
545 0210	4.1	0.8
479 0080	21.2	1.3
355 0260	6.9	0.7
479 0200	21.5	1.3
416 0250	1.6	0.6
031 0050	8.4	0.9
302 0070	6.0	1.0
549 0220	7.1	1.1
201 0220	4.3	1.0
551 0130	22.3	1.6
287 0460	14.2	0.8
600 0070	10.1	2.8
343 0280	22.7	2.9
237 0300	8.6	0.7
601 0120	4.2	0.5
108 0200	5.8	0.7
405 0180	19.0	1.0
290 0350	5.2	0.8
290 0450	63.8	2.5
407 0140	33.6	2.1
605 0070	44.9	1.7
606 0110	3.0	0.8
293 0270	25.8	1.2

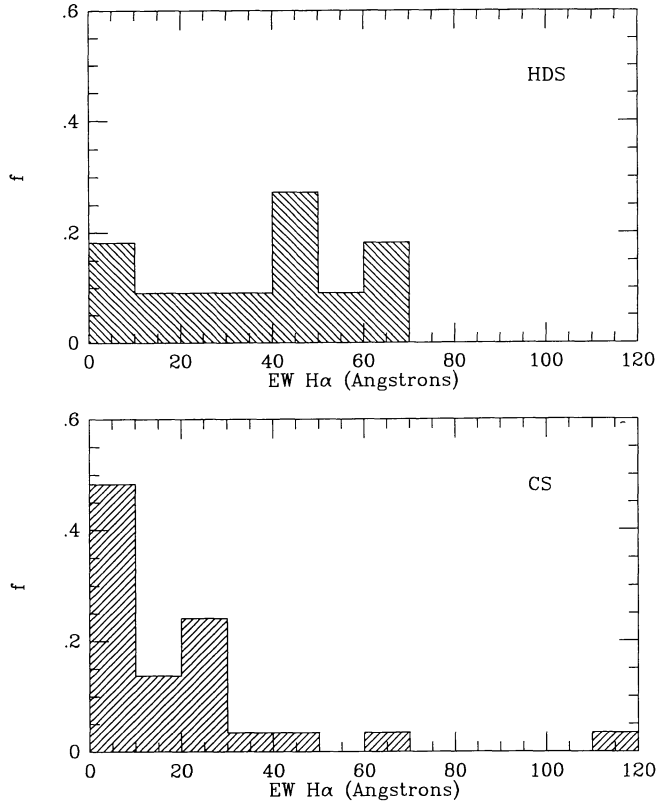

FIG. 4.—Frequency distribution of Hα emission-line equivalent widths for HDS and CS samples.

Column (7): H I mass-to-light ratio $M_{\rm H\,I}/L_B$, in solar units, assuming a solar photographic absolute magnitude of +5.37.

Column (8): The reference from which the radio fluxes were obtained to derive the physical parameters described above.

The H I characteristics of both samples can be compared in the plots of Figure 5 where $M_{\rm H\,I}$ (upper panels), $\sigma_{\rm H\,I}$ (middle panels), and $M_{\rm H\,I}/L_B$ (lower panels) are displayed for CS (left panels) and HDS (right panels) samples as a function of the morphological type. The width of the distribution is much larger in the HDS $M_{\rm H\,I}$ plot, indeed suggesting that in dense regions many galaxies attain low $M_{\rm H\,I}$ content. The comparison of the $\sigma_{\rm H\,I}$ distributions also provide some evidence of the gas depletion phenomenon in the HDS sample. In addition to the morphological dependence, the H I galaxy content also presents some luminosity dependence for a same morphological class; the $M_{\rm H\,I}/L_B$ ratio is expected to minimize this effect. The result is that the HDS sample clearly shows a deficiency of H I content when compared to the control sample CS. This effect is present in density regimes lower than those found in clusters where anemic galaxies are usually found, suggesting that it spans a wider density range, as does also the morphology-density phenomenon. The number of galaxies with radio information is still low, but the results are encouraging to pursue the investigation.

3.3. *Far-Infrared*

The far-infrared (FIR) radiation turned out to be an important tool in the diagnostics of starburst activity in galaxies, and

1994ApJS...93..425M

TABLE 5

21 CM INFORMATION FOR THE HDS SAMPLE

ESO	Type	D_B	F_c	logM_{HI}	logσ_{HI}	M_{HI}/L_B	Ref.
409 0220	6.0	2.70	21.17	8.89	11.28	1.29	1
150 0050	8.0	4.30	15.67	8.65	10.51	1.05	1
475 0140	9.0	2.70	17.18	9.69	12.93	2.00	1
152 0240	6.0	5.00	40.77	8.97	11.67	0.43	2
013 0280	4.0	2.40	15.67	9.83	15.91	3.47	1
478 0060	4.0	2.20	13.39	9.90	14.24	0.43	1
478 0280	9.0	1.90	21.98	9.60	16.17	0.37	3
545 0210	5.0	2.80	22.06	10.06	16.99	0.85	1
355 0260	4.0	1.90	5.43	8.56	6.78	0.30	1
355 0300	4.0	2.50	16.06	9.83	17.47	0.74	1
416 0250	3.0	2.40	12.79	9.81	8.19	1.63	1
357 0130	5.0	2.50	7.11	9.47	3.79	0.16	2
083 0060	4.3	2.40	9.98	9.78	22.17	1.67	1
031 0200	4.3	1.80	11.03	9.72	26.88	1.69	1
083 0100	6.0	2.00	3.28	9.32	6.97	0.55	1
302 0070	5.0	2.00	7.48	9.71	23.47	1.25	1
550 0050	8.5	3.02	15.55	8.97	14.07	1.98	1
201 0220	5.0	2.90	13.38	9.63	7.47	1.70	1
551 0300	7.0	2.09	5.00	9.26	14.98	0.76	4
422 0270	5.0	1.80	6.53	9.38	11.52	0.52	1
305 0140	5.0	1.70	6.79	9.52	14.74	0.50	1
204 0190	6.0	2.00	9.26	9.59	15.96	1.29	1
142 0500	5.0	6.00	60.10	9.72	16.05	0.84	1
074 0190	1.0	2.10	8.45	9.51	5.42	0.56	1
107 0160	8.0	3.20	18.18	9.04	11.38	3.67	1
145 0050	7.0	4.40	73.67	9.39	22.59	1.24	1
287 0460	6.0	1.90	13.65	9.83	24.65	1.20	1
188 0170	4.8	2.90	6.38	9.14	6.78	0.35	1
237 0020	4.5	3.70	16.31	9.97	8.30	0.57	1
075 0370	6.5	2.40	6.69	9.33	5.04	1.35	1
532 0090	5.0	2.00	21.78	9.48	20.64	0.70	2
237 0270	10.0	6.00	94.16	5.35	13.82	0.40	2
146 0090	5.0	4.00	35.00	9.21	9.14	0.31	1
532 0220	5.4	1.70	15.31	9.20	21.46	1.95	1
146 0140	7.0	3.20	17.57	8.95	5.77	3.55	1
108 0200	3.9	4.80	60.54	9.48	13.76	2.55	1
289 0180	8.0	11.00	178.71	9.28	14.42	1.19	1
467 0490	3.0	1.80	11.44	9.56	17.59	0.70	1
109 0210	7.0	4.40	27.85	9.44	8.35	2.69	1
290 0350	4.7	2.50	9.21	9.83	8.15	1.70	1
407 0140	5.0	2.40	13.00	9.28	16.24	0.55	1
292 0140	5.0	3.00	14.71	8.76	6.83	0.98	1
149 0010	7.8	5.00	1.20	7.75	0.39	0.05	2
471 0200	4.5	3.80	45.25	9.89	12.37	0.52	1

References for 21 cm data: 1: Mathewson et al. 1992; 2: Huchtmeier and Richter 1989b; 3: Fisher & Tully 1981; 4: Fouqué et al. 1990.

TABLE 6

21 CM INFORMATION FOR THE CS SAMPLE

ESO	Type	D_B	F_c	logM_{HI}	logσ_{HI}	M_{HI}/L_B	Ref.
352 0460	8.0	2.30	7.94	9.30	8.64	0.70	1
352 0470	10.0	1.60	2.40	8.84	9.27	0.58	4
153 0170	5.0	3.30	15.23	10.14	20.86	0.93	1
545 0070	10.0	1.80	64.40	9.38	86.21	1.88	3
545 0110	5.0	5.80	55.00	9.27	5.59	0.23	3
548 0070	3.5	4.50	28.29	9.04	4.77	0.40	3
548 0100	7.0	2.70	5.70	8.13	5.66	0.20	2
358 0090	3.3	3.00	8.01	8.27	3.80	0.64	1
548 0310	3.0	3.20	9.12	8.54	2.61	0.10	2
358 0150	9.0	1.60	1.70	7.76	5.09	0.38	4
548 0380	6.0	2.80	13.57	8.88	7.57	0.21	1
548 0390	9.0	1.95	37.06	9.39	21.16	0.68	1
358 0170	3.0	14.00	185.79	9.86	8.43	0.34	1
482 0330	0.0	3.63	7.80	8.46	2.81	0.13	2
549 0020	10.0	1.70	1.80	7.47	7.11	0.25	4
358 0540	8.0	2.40	6.00	7.62	6.84	0.37	3
358 0580	3.0	3.50	25.07	8.56	10.13	0.42	2
358 0610	10.0	3.20	8.84	8.44	5.54	0.59	2
157 0050	5.0	2.40	9.12	8.27	6.26	0.32	2
157 0180	6.0	3.30	20.88	8.69	7.70	1.27	1
157 0320	9.0	2.40	11.20	8.57	12.19	0.62	2
118 0430	4.0	9.00	209.10	9.68	19.37	0.56	2
119 0060	7.5	3.00	16.75	8.48	9.79	0.31	1
119 0190	5.0	4.50	17.90	8.75	8.50	0.25	2
305 0060	3.4	8.00	47.42	8.93	5.66	0.15	1
305 0080	1.0	10.00	66.19	8.81	8.66	0.23	2
362 0060	6.0	3.50	27.53	8.52	8.84	0.97	3
284 0290	4.0	2.20	6.25	9.60	6.65	0.42	1
285 0050	5.0	1.80	13.30	9.40	22.41	1.07	2
234 0220	4.0	1.80	9.73	9.85	11.61	0.41	1
285 0080	4.0	9.00	47.50	9.89	10.31	0.42	2
288 0260	5.0	3.70	19.58	9.29	9.09	0.75	2
288 0280	9.0	3.90	23.87	9.38	14.61	1.01	1
404 0270	4.7	3.50	12.58	9.22	9.47	0.48	1
108 0110	3.3	2.10	8.23	9.14	7.80	0.32	1
467 0070	0.0	2.10	2.30	8.46	2.81	0.11	2
467 0081	3.0	2.00	2.51	8.53	8.85	0.27	2
467 0082	3.5	2.05	2.49	8.53	35.77	0.38	2
289 0080	1.0	1.80	23.51	9.15	25.00	0.57	2
289 0070	9.0	3.00	8.50	8.73	3.28	0.16	2
289 0090	9.0	2.00	20.52	9.20	25.05	0.87	3
406 0260	6.0	5.50	23.85	9.05	5.18	1.01	3
406 0250	5.0	4.60	26.99	8.96	5.47	0.22	1
406 0270	7.0	3.60	20.30	9.19	21.09	1.24	4
406 0290	1.8	2.70	25.42	9.29	15.20	1.07	1
290 0290	1.0	8.00	58.90	9.47	6.26	0.30	2
406 0330	6.0	4.00	52.59	9.51	16.13	1.40	1
291 0120	2.5	4.50	40.79	9.22	9.94	0.21	3
291 0160	1.0	8.00	48.05	9.28	3.62	0.19	2
347 0330	3.0	2.90	65.64	9.37	28.44	0.76	2
347 0340	3.0	5.00	38.22	9.26	6.29	0.37	1
240 0110	4.8	7.00	63.58	9.98	7.41	1.86	1

References for 21 cm data are the same as in Table 5.

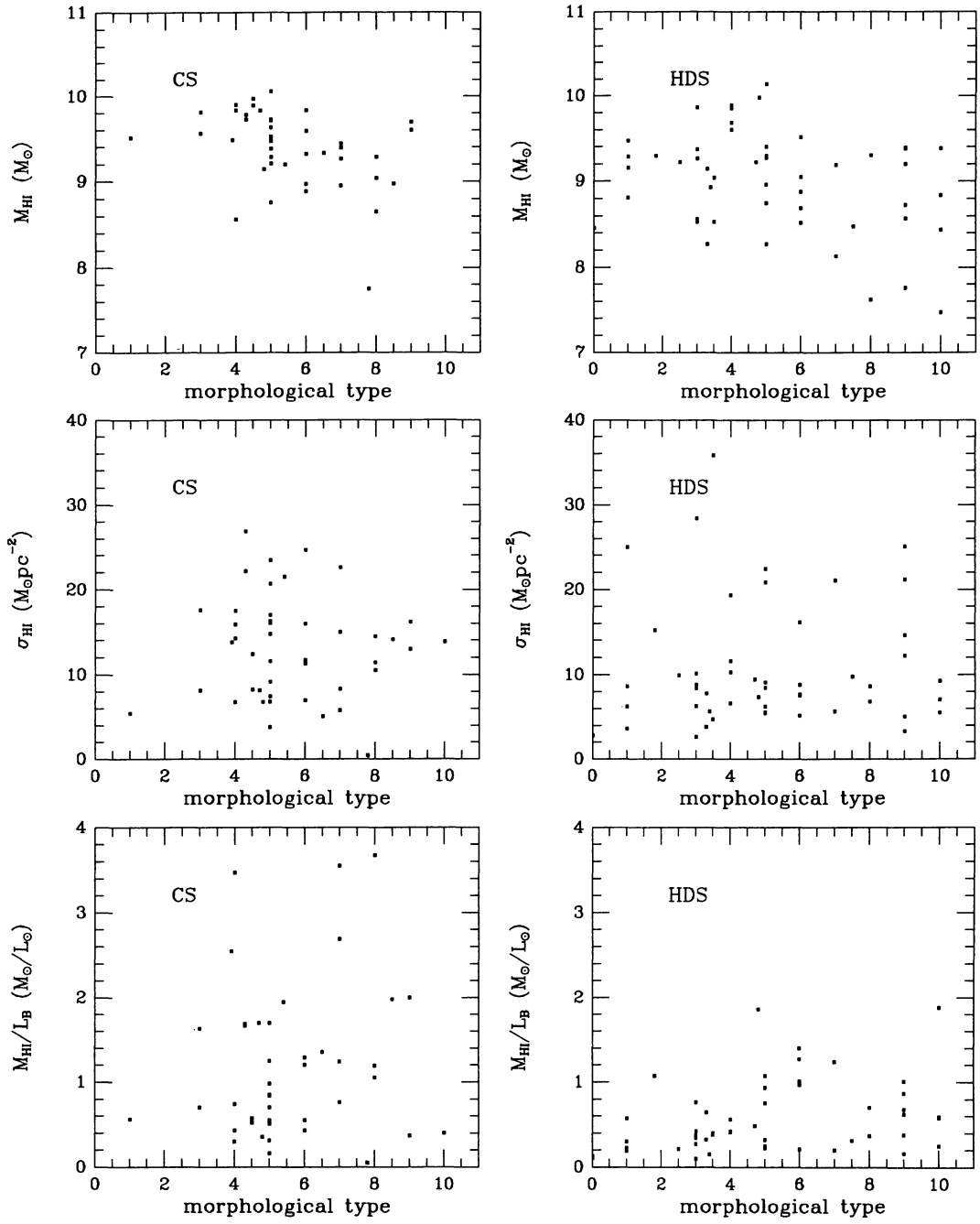

FIG. 5.—H I mass (*upper panels*), pseudo H I surface density (*middle panels*), and H I mass-to-luminosity ratio (*lower panels*) as a function of morphological type for CS (*left panels*) and HDS (*right panels*) samples.

the *IRAS* survey provides a large database for this purpose. Some details about modeling FIR radiation are still subject of debate. While some authors claim that the FIR emission comes from the star-forming regions only (e.g., Devereux & Young 1990), others have proposed a two-component model made up by a star-forming region and a quiescent cirrus-like region of the interstellar medium (e.g., Helou 1986; Rowan-Robinson, & Crawford 1989). Some large optically selected samples such as the one taken from the *Uppsala General Catalog of Galaxies* (Bothun, Lonsdale, & Rice 1989), or the Center for Astrophysics magnitude-limited sample ($m_B \leq 14.5$) by Thuan & Sauvage (1992) revealed some global properties of galaxies in the FIR region. Our purpose is to provide with the characteristics of our two samples in the far-infrared region. In order to achieve this goal we used the *IRAS Point Source Catalog* (version 2.0) (PSC), to extract the information at 12, 25, 60,

TABLE 7

INFRARED DATA FOR GALAXIES IN THE HDS SAMPLE

ESO	Type	f_{12}	f_{25}	f_{60}	f_{100}	C_0	C_1	C_2	C_3	α_{25}^{60}	α_{60}^{100}	$\log L_{FIR}$	ET
353 0060	2.0	0.250	0.514	3.471	5.529	0	0	2	10	-2.18	-0.91	10.23	1
297 0080	1.5	0.285	0.250	0.465	1.204	0	1	4	10	-0.71	-1.86	9.38	5
153 0170	5.0	0.250	0.250	0.408	1.251	0	2	2	10	-0.56	-2.19	9.54	5
153 0200	3.0	0.321	0.231	0.900	2.534	0	2	2	10	-1.55	-2.03	9.77	4
545 0070	10.0	0.250	0.338	1.960	3.712	0	0	5	10	-2.01	-1.25	8.74	5
545 0100	5.0	0.521	0.303	2.486	5.504	0	0	4	11	-2.40	-1.56	8.98	5
545 0110	5.0	0.913	1.253	13.860	44.430	4	0	1	11	-2.75	-2.28	9.66	5
546 0150	3.0	0.250	0.335	1.059	3.126	0	0	1	11	-1.32	-2.12	10.09	2
357 0190	5.0	0.312	0.250	0.921	3.238	0	0	4	10	-1.49	-2.46	8.64	5
357 0230	0.0	0.346	0.269	3.583	9.704	0	0	2	10	-2.96	-1.95	9.25	3
357 0220	-2.0	0.289	0.286	3.077	7.694	0	0	3	10	-2.72	-1.79	9.07	5
548 0070	3.5	0.250	0.298	0.837	3.479	0	0	1	11	-1.18	-2.79	8.56	5
548 0180	-3.0	0.250	0.250	0.517	1.804	0	0	2	11	-0.83	-2.45	8.22	5
548 0310	3.0	0.288	0.259	2.676	8.254	0	0	1	11	-2.67	-2.21	8.98	5
548 0380	6.0	0.250	0.931	8.685	11.480	0	0	1	11	-2.55	-0.55	9.51	5
548 0390	9.0	0.250	0.253	2.113	4.098	0	2	3	12	-2.42	-1.30	9.02	5
358 0170	3.0	3.212	11.090	78.150	141.500	0	1	1	10	-2.23	-1.16	10.35	4
548 0510	-2.0	0.412	1.912	7.228	5.955	0	0	1	11	-1.52	0.38	9.33	3
358 0280	-3.0	0.250	0.250	1.047	2.962	0	0	3	10	-1.64	-2.04	8.71	5
358 0350	-2.0	0.503	1.441	5.886	9.917	0	1	1	9	-1.61	-1.02	8.51	4
358 0360	-2.0	0.250	0.276	2.311	5.956	0	0	1	9	-2.43	-1.85	8.63	5
482 0330	0.0	0.256	0.549	5.277	12.320	0	1	1	10	-2.58	-1.66	9.20	5
548 0770	2.0	0.250	0.250	0.444	1.157	0	1	5	10	-0.66	-1.87	8.19	5
358 0580	3.0	0.250	0.250	0.539	2.869	0	0	2	9	-0.88	-3.27	8.02	2
358 0610	10.0	0.250	0.250	0.400	1.196	0	2	5	10	-0.54	-2.14	8.07	2
157 0050	5.0	0.250	0.250	0.462	1.880	4	1	4	10	-0.70	-2.75	8.03	5
157 0120	-1.0	0.610	0.762	7.165	22.700	4	1	1	9	-2.56	-2.26	9.01	5
157 0170	-3.0	0.314	0.250	0.518	0.809	0	2	5	10	-0.83	-0.87	7.86	5
157 0180	6.0	0.250	0.250	0.511	1.708	0	2	4	9	-0.82	-2.36	8.07	5
157 0260	-3.0	0.289	0.456	0.941	2.118	0	1	4	11	-0.83	-1.59	8.44	5
157 0320	9.0	0.250	0.250	1.045	2.221	0	1	2	9	-1.63	-1.48	8.43	5
118 0430	4.0	1.470	4.034	34.800	69.460	4	3	1	10	-2.46	-1.35	9.79	4
119 0060	7.5	0.252	0.265	2.673	6.575	0	1	3	11	-2.64	-1.76	8.61	5
119 0190	5.0	0.250	0.221	2.049	8.026	0	1	2	10	-2.55	-2.67	8.85	5
305 0060	3.4	1.352	1.846	25.350	74.810	8	0	1	10	-2.99	-2.12	9.63	5
305 0080	1.0	4.121	15.870	97.120	136.500	0	1	1	10	-2.07	-0.67	9.80	4
362 0060	6.0	0.250	0.315	0.859	2.197	0	0	5	10	-1.14	-1.84	7.95	5
119 0540	0.0	0.361	0.250	0.348	1.477	0	2	3	11	-0.38	-2.83	9.34	5
233 0320	-5.0	0.250	0.250	1.016	3.276	0	1	3	18	-1.60	-2.29	9.21	3
233 0410	2.0	0.250	0.276	0.643	2.372	0	2	3	15	-0.97	-2.56	8.98	5
284 0320	0.0	0.250	0.508	3.580	5.389	0	1	4	15	-2.23	-0.80	10.26	1
284 0310	4.0	0.250	0.271	1.204	4.193	0	1	4	15	-1.71	-2.44	9.97	3
234 0130	4.0	0.250	0.250	0.756	2.209	0	2	4	14	-1.26	-2.10	9.55	2
285 0070	-0.7	0.299	0.660	5.037	6.700	0	0	2	14	-2.32	-0.56	9.77	1
234 0220	4.0	0.254	0.250	1.796	5.154	0	1	2	15	-2.25	-2.06	10.07	2
285 0080	4.0	0.250	0.252	0.809	4.084	0	0	3	16	-1.33	-3.17	9.22	5
235 0550	5.0	0.250	0.250	0.431	2.317	8	0	3	12	-0.62	-3.29	9.50	3
288 0260	5.0	0.268	0.373	0.497	1.551	0	1	2	11	-0.33	-2.23	8.68	5
466 0380	1.0	0.457	0.777	5.958	12.850	0	0	2	17	-2.33	-1.50	9.80	4
466 0400	-0.5	0.250	0.268	3.490	8.074	0	1	3	17	-2.93	-1.64	9.66	5
404 0270	4.7	0.250	0.262	0.602	1.409	0	2	3	14	-0.95	-1.66	8.81	2
108 0130	3.5	0.250	0.250	0.563	2.119	0	0	3	11	-0.93	-2.59	9.00	5
467 0081	3.0	0.250	0.356	2.355	4.485	0	0	2	15	-2.16	-1.26	9.38	5
289 0080	1.0	0.600	0.888	4.046	6.622	0	0	2	11	-1.73	-0.96	9.24	5
406 0250	5.0	0.287	0.497	3.881	15.380	0	1	1	10	-2.35	-2.70	9.16	5
406 0290	1.8	0.250	0.250	0.513	2.391	0	1	3	10	-0.82	-3.01	8.68	5
346 0170	4.5	0.250	0.250	1.002	3.099	0	1	3	11	-1.59	-2.21	8.75	3
406 0300	-5.0	1.208	0.250	0.421	1.039	0	1	4	10	-0.60	-1.77	8.20	2
290 0290	1.0	0.289	0.250	0.888	5.835	0	0	1	10	-1.45	-3.69	8.83	5
406 0330	6.0	0.291	0.490	3.129	8.971	0	0	1	10	-2.12	-2.06	9.25	2
291 0120	2.5	2.981	11.960	72.930	100.900	0	0	1	9	-2.07	-0.64	10.30	4
291 0160	1.0	1.350	6.329	48.010	72.760	4	0	2	9	-2.31	-0.81	10.12	4
347 0330	3.0	0.517	0.844	7.385	18.020	0	0	3	9	-2.48	-1.75	9.35	4
347 0340	3.0	0.523	0.621	6.125	18.280	0	0	3	9	-2.61	-2.14	9.43	2
240 0110	4.8	0.250	0.250	0.917	5.179	0	0	1	9	-1.48	-3.39	9.28	3
240 0130	3.0	0.250	0.214	1.256	2.837	0	0	2	9	-2.02	-1.60	9.32	5

1994ApJS...93..425M

TABLE 8

INFRARED DATA FOR GALAXIES IN THE CS SAMPLE

ESO	Type	f_{12}	f_{25}	f_{60}	f_{100}	C_0	C_1	C_2	C_3	α_{25}^{60}	α_{60}^{100}	$\log L_{FIR}$	ET
539 0050	5.0	0.250	0.250	0.912	2.965	0	0	1	13	-1.48	-2.31	9.26	5
350 0140	6.0	0.696	0.250	0.563	1.823	0	0	1	13	-0.93	-2.30	9.10	2
079 0020	7.1	0.293	0.250	0.448	1.048	0	0	4	9	-0.67	-1.66	8.71	5
411 0010	0.0	0.485	1.307	11.520	19.620	0	1	1	10	-2.49	-1.04	10.30	5
079 0070	8.0	0.250	0.250	1.096	2.308	0	1	3	12	-1.69	-1.46	9.90	5
541 0010	3.5	0.570	0.318	0.299	1.462	0	1	3	12	0.07	-3.11	9.51	5
051 0110	3.0	0.250	0.258	0.912	2.235	0	0	1	11	-1.44	-1.76	9.90	2
013 0120	-3.0	0.263	0.250	1.541	6.191	0	0	2	12	-2.08	-2.72	9.79	5
114 0010	5.6	0.250	0.250	0.400	1.049	0	1	4	10	-0.54	-1.89	9.33	5
244 0440	1.0	0.250	0.250	2.120	4.183	0	1	1	9	-2.44	-1.33	10.19	5
152 0240	6.0	0.250	0.572	1.331	5.832	0	0	1	10	-0.97	-2.89	8.55	5
297 0370	4.7	0.261	0.250	0.430	1.470	0	1	3	9	-0.62	-2.41	9.43	5
477 0180	4.0	0.250	0.299	1.245	3.806	0	0	2	10	-1.63	-2.19	9.70	5
013 0280	4.0	0.250	0.250	1.078	3.590	0	3	4	13	-1.67	-2.36	9.66	5
478 0020	3.5	0.414	0.252	0.649	1.645	0	1	2	10	-1.08	-1.82	9.35	5
478 0060	4.0	0.350	0.458	3.306	9.813	0	0	1	10	-2.26	-2.13	10.26	5
478 0280	9.0	0.249	0.425	5.200	9.777	0	0	1	9	-2.86	-1.24	9.85	5
355 0260	4.0	0.343	0.250	0.511	1.609	0	1	3	10	-0.82	-2.24	8.51	2
355 0300	4.0	0.437	0.250	0.922	3.262	0	1	3	10	-1.49	-2.47	9.60	3
115 0280	4.0	0.250	0.250	0.573	2.104	0	2	3	10	-0.95	-2.55	9.72	5
417 0080	0.5	0.250	0.272	2.287	4.721	0	0	2	10	-2.43	-1.42	9.94	1
031 0050	3.5	0.250	0.274	1.075	3.818	0	0	2	10	-1.56	-2.48	9.72	2
357 0130	5.0	0.250	0.271	0.752	3.216	0	0	3	9	-1.17	-2.84	9.55	5
482 0010	3.0	0.255	0.250	0.555	1.480	0	0	2	10	-0.91	-1.92	9.27	5
419 0030	4.0	0.250	0.250	1.350	3.205	0	0	2	9	-1.93	-1.69	9.59	5
482 0430	4.0	0.284	0.250	0.656	2.423	4	1	2	10	-1.10	-2.56	9.39	5
483 0060	3.0	0.261	0.256	0.468	1.075	0	1	4	11	-0.69	-1.63	9.12	5
420 0030	5.0	0.250	0.250	0.678	2.388	0	0	2	9	-1.14	-2.46	9.37	5
201 0220	5.0	1.049	0.250	0.786	1.045	0	2	3	9	-1.31	-0.56	9.22	3
202 0140	1.0	0.250	0.250	0.939	2.547	4	0	2	10	-1.51	-1.95	9.82	5
118 0230	5.0	0.333	0.250	0.400	1.031	0	1	3	10	-0.54	-1.85	9.56	5
484 0250	2.0	0.288	0.323	2.009	4.868	0	1	3	11	-2.09	-1.73	9.76	5
551 0130	6.0	0.250	0.658	0.467	1.523	0	1	4	11	0.39	-2.31	9.60	2
485 0060	6.0	0.250	0.250	0.424	0.883	0	1	4	12	-0.60	-1.44	9.12	5
485 0120	5.0	0.250	0.250	0.327	1.377	0	1	3	11	-0.31	-2.81	9.20	5
361 0190	1.0	0.250	0.587	0.697	0.994	0	0	4	10	-0.20	-0.70	8.66	1
422 0120	4.0	0.250	0.250	0.503	2.102	0	0	2	11	-0.80	-2.80	9.46	5
203 0180	4.0	1.069	0.211	2.553	8.110	0	0	1	9	-2.85	-2.26	9.90	5
486 0400	3.0	0.351	0.250	0.368	1.121	0	0	4	11	-0.44	-2.18	9.39	5
159 0230	3.0	0.250	0.250	0.448	2.048	0	4	4	14	-0.67	-2.97	9.77	5
160 0020	2.5	0.290	0.385	2.802	6.705	0	1	3	15	-2.27	-1.71	9.99	5
142 0500	5.0	0.250	0.250	1.752	6.158	0	0	3	14	-2.22	-2.46	9.19	5
106 0120	6.0	0.250	0.250	0.665	2.502	0	0	2	12	-1.12	-2.59	9.41	5
342 0350	1.0	0.468	0.250	0.541	1.107	0	0	4	14	-0.88	-1.40	9.10	2
145 0050	7.0	0.250	0.250	1.911	5.205	0	1	2	14	-2.32	-1.96	8.75	1
237 0020	4.5	0.250	0.250	0.758	3.441	0	0	2	11	-1.27	-2.96	9.72	5
466 0110	-3.0	0.250	0.250	0.735	2.288	0	1	2	15	-1.23	-2.22	9.65	3
189 0070	4.0	0.250	0.184	2.048	6.164	0	0	2	9	-2.75	-2.16	9.53	5
145 0220	4.5	0.368	0.250	0.983	3.229	0	0	3	12	-1.56	-2.33	9.61	3
532 0090	5.0	0.250	0.290	1.271	3.532	0	1	3	17	-1.69	-2.00	9.20	5
237 0270	10.0	0.250	0.250	2.349	6.814	0	0	3	11	-2.56	-2.08	4.71	5
601 0120	3.0	0.250	0.321	0.489	1.490	0	2	6	18	-0.48	-2.18	9.47	2
146 0090	5.0	0.596	0.855	9.098	23.920	8	1	1	11	-2.70	-1.89	9.57	5
108 0200	3.9	0.375	0.309	3.350	10.840	0	0	1	10	-2.72	-2.30	9.21	1
533 0060	3.0	0.250	0.250	0.718	1.224	0	0	5	15	-1.21	-1.04	9.77	5
289 0180	8.0	0.250	0.250	0.333	3.253	0	1	4	11	-0.33	-4.46	7.86	5
146 0200	5.0	0.675	0.250	0.638	1.433	0	2	2	11	-1.07	-1.59	9.39	5
467 0490	3.0	0.250	0.431	0.571	1.764	0	0	3	13	-0.32	-2.21	9.24	5
405 0180	1.0	0.264	0.503	2.091	5.388	0	0	1	14	-1.63	-1.85	9.62	1
238 0240	3.0	0.250	0.682	0.355	1.604	0	0	2	11	0.75	-2.95	9.66	5
407 0140	5.0	0.250	0.250	1.022	2.749	0	0	2	10	-1.61	-1.94	9.13	2
605 0070	3.0	0.661	0.315	0.807	1.665	0	0	2	16	-1.07	-1.42	9.03	1
292 0140	5.0	0.250	0.299	0.782	1.661	0	1	2	8	-1.10	-1.47	8.38	5
149 0010	7.8	0.250	0.250	0.602	1.358	0	0	3	11	-1.00	-1.59	8.36	2
471 0200	4.5	0.348	0.293	2.787	8.112	0	0	0	-1	-2.57	-2.09	9.65	5
012 0120	4.0	0.250	0.250	0.637	2.338	0	2	3	13	-1.07	-2.55	9.96	5

and 100 μm. The galaxies of our samples detected by *IRAS* are shown in Tables 7 (HDS sample) and 8 (CS sample) which contain:

Column (1): The ESO-Uppsala name (as given in Tables 1 and 2).

Column (2): The morphological type (also as given in Tables 1 and 2).

Columns (3)–(6): Flux densities f_{12}, f_{25}, f_{60}, and f_{100}, in janskys, respectively, for 12, 25, 60, and 100 μm bands.

Column (7): *IRAS* confusion flag, C_0, hex-encoded according to the PSC.

Columns (8)–(10): *IRAS* PSC cirrus flags CIRR1, CIRR2, and CIRR3, denoted in the table by C_1, C_2, and C_3, respectively.

Column (11) and (12): Spectral indices α_{25}^{60} and α_{60}^{100}.

Column (13): Total far-infrared luminosity between $\sim$40 μm and $\sim$120 μm, $L_{\rm FIR}$, in $L_\odot$, computed following Lonsdale et al. (1985):

$$L_{\rm FIR} = 3.95 \times 10^5 (2.58 f_{60} + f_{100}) \times d^2 ,$$

where d is the distance in Mpc.

Column (14): Emission-line type code (EL) as described in the text.

The distribution of $L_{\rm FIR}$ against morphological type is displayed in Figure 6 for both samples. The HDS sample presents a low infrared-luminosity population due to early-type galaxies, which is natural since we have a higher fraction of these galaxies in this sample. In this figure we display galaxies with spectrum available in the SSRS database (except for Seyferts; see details in the next section), which enabled us to classify them according to the emission-line (EL) characteristics. The EL classes are: (1) objects with emission lines typical of galaxies with starburst activity; (2) objects with weak emission lines (probably very low or no current starburst activity); (3) objects with no emission lines; (4) Seyfert galaxies (present only in the HDS sample); and (5) objects with no spectral information in the SSRS database. The far-infrared most luminous objects of the HDS sample are Seyfert and starburst galaxies. In the CS sample, there is no optical spectral information for the far-infrared most luminous galaxies, but since the Seyfert population was checked in the Véron-Cetty & Véron (1991) catalog, these objects are more probably galaxies with starburst characteristics. The CS presents a higher fraction of galaxies with weak emission lines, suggesting that the HDS sample has more galaxies with current strong starburst activity than the CS, reinforcing the findings from the Hα emission line.

The distribution of spectral indices $\alpha(100, 60)$ against $\alpha(60, 25)$ for the two samples is presented in Figure 7, where the symbols have the same meaning as in Figure 6. In particular, the Seyfert galaxies (HDS) do not present a trend for flatter spectra at shorter wavelengths, where the power-law component tends to dominate. This supports the idea that the Seyferts detected in the infrared may have a substantial contribution of nuclear starburst activity, and the latter would be enhanced by

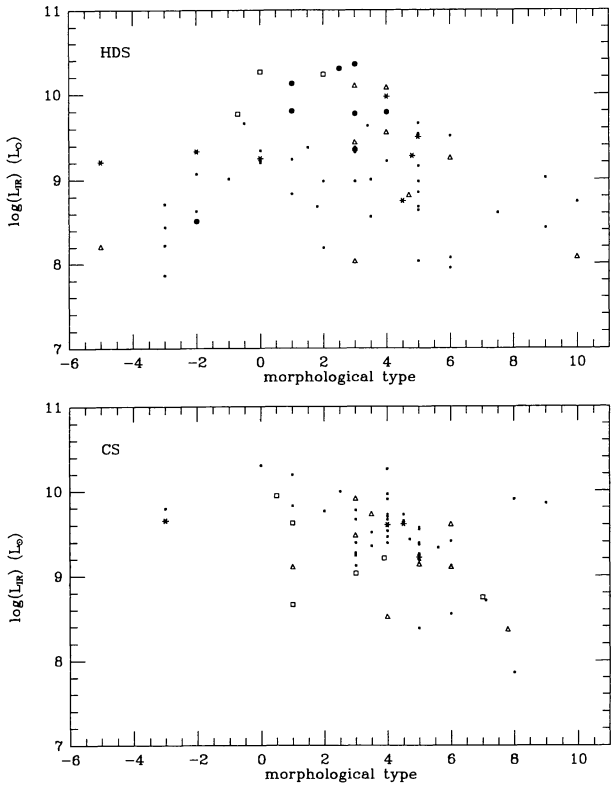

FIG. 6.—Logarithm of $L_{\rm FIR}$ in $L_\odot$ vs. morphological type. *Empty squares:* starburst galaxies; *empty triangles:* galaxies with weak emission lines; *asterisks:* objects with no emission lines; *filled circles:* Seyferts; *dots:* galaxies without spectral information.

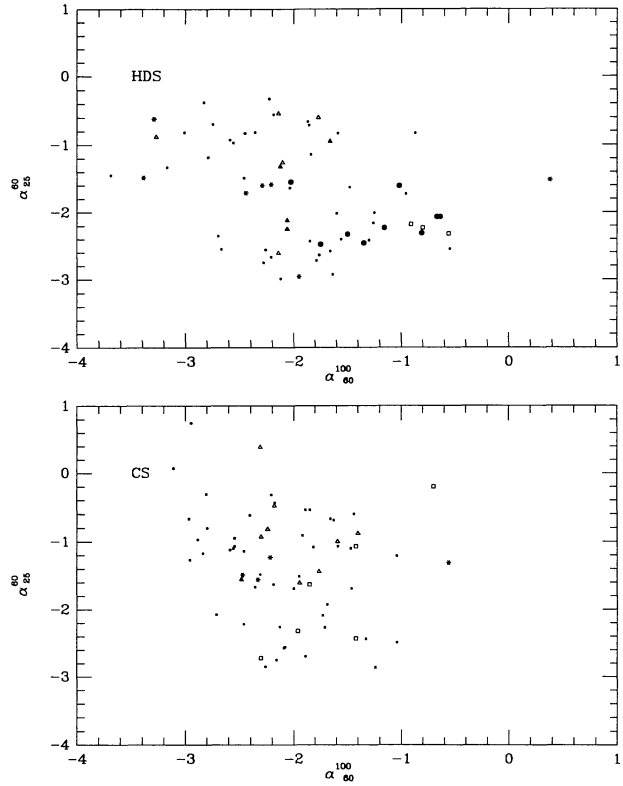

FIG. 7.—Infrared spectral indices for HDS and CS samples. The symbols are as in Fig. 6.

the environment rather than by the nonthermal-powered activity.

3.4. *Seyfert Activity*

Several investigations of possible environmental effects on Seyfert activity have been made (e.g., MacKenty 1989; Dahari 1984, 1985; Fuentes-Williams & Stocke 1988), but the emphasis was mainly on the existence and nature of possible Seyfert companions. Our goal is rather to examine the frequency of the Seyfert phenomenon in samples that were selected with objective criteria based on the local density of objects. We have checked all the objects in our HDS and CS samples for their possible inclusion in the Véron-Cetty & Véron's (1991) AGN catalog. This catalog is not complete in any sense, since it is a compilation from the information of the literature. Also, the SSRS spectral database was searched for the possible presence of Seyfert galaxies. The lack of complete information does not allow us to set some possible selection effects on the results, but they can be considered as preliminary, up to the moment that we have obtained spectra for the whole galaxies of our samples. The result is that only the HDS sample was found to have Seyfert galaxies. These galaxies are listed in Table 9, with the following information:

Column (1): ESO name, as in Table 1.
Column (2) and (3): Right ascension and declination 1950.
Column (4): Morphological type.
Column (5): Seyfert class, where S1, S2, and S stand for Seyferts type 1, 2, and unclear type, according to Véron-Cetty & Véron (1991).

There appears to exist a clear preference for Seyferts to be present in high local density environments, or at least a subsample of Seyferts that have also nuclear starburst contribution as seen in the previous section. More optical spectral information is necessary to clarify this point.

3.5. *Presence of Bars in Spiral Galaxies*

High-density environments favor close encounters between galaxies, a possible mechanism for triggering bars in spiral disks as indicated in *N*-body simulations (e.g., Noguchi 1987). Giuricin et al. (1993) searched for the presence of bar structures in a sample of nearby spiral galaxies, and confirmed this tendency at a good confidence level. We checked our two samples for the presence of barred galaxies among the morphological types Sa to Sc using information given by Lauberts (1982). We found 15% and 11% of barred galaxies, respectively, for the HDS and CS samples in this subgroup of morphological types, which indeed suggests some trend.

TABLE 9

ACTIVE GALAXIES IN HDS SAMPLE

ESO	R.A.	Decl.	Type	Class
153 0200	020420	−552547	3.0	S2
358 0170	033141	−361824	3.0	S1
358 0350	033452	−360948	−2.0	S2
118 0430	044454	−592000	4.0	S
305 0080	050559	−373400	1.0	S
466 0380	215906	−320627	1.0	S2
291 0160	231536	−423835	1.0	S2
347 0330	231612	−423100	3.0	S2

4. CONCLUSIONS

We have generated galaxy samples in high- and in a low-density environments, using objective criteria applied to the SSRS database. The samples will be used as targets for detailed spectroscopic analyses of the emission-line spectrum and of the stellar population. In this work we studied their global physical properties. The main findings may be summarized as follows:

The samples respect the morphology-density relation, that is, the high-density sample contains a high percentage of early-type galaxies.

The available Hα emission-line information suggests that the high-density sample galaxies are more prone to starburst activity, probably enhanced by nearby galaxies.

The H I content of galaxies in the high-density sample is lower when globally compared to that of galaxies in the low-density one; this is similar to, although not with the strength of, the effect already found in the core of clusters of galaxies. The phenomena may have a continuous behavior as a function of density, like the one for the morphology-density relation.

The far-infrared data also point to a more intense starburst activity in the high-density sample.

Seyfert activity was detected only in the high-density sample.

Barred galaxies among the Sa to Sc spirals are more numerous in the high-density sample.

More detailed spectral analyses are necessary to check some of these results further. Optical spectral observations of spirals are under way, and a more complete and detailed analysis is the subject of forthcoming papers. Results of a preliminary subsample are presented by Pastoriza et al. (1993).

M.A.G.M. acknowledges CNPq grant 301366/86-1 for partially support of this project.

REFERENCES

Bothun, G. D., Lonsdale, C. J., & Rice, W. 1989, ApJ, 341, 129
Bushouse, H. A. 1986, AJ, 91, 255
da Costa, L. N., Pellegrini, P. S., Davis, M., Meiksin, A., Sargent, W. L. W., & Tonry, J. 1991, ApJS, 75, 935
da Costa, L. N., et al. 1988, ApJ, 327, 544
da Costa, L. N., Pellegrini, P. S., Willmer, C., de Carvalho, R., Maia, M., Latham, D. W., & Geary, J. C. 1989, AJ, 97, 315
Dahari, O. 1984, AJ, 89, 966
———. 1985, AJ, 90, 1772
Devereux, N. A., & Young, J. S. 1990, ApJ, 350, L25
Dressler, A. 1980, ApJ, 236, 351
———. 1984, ARA&A, 22, 185
Fisher, J. R., & Tully, R. B. 1981, ApJS, 47, 139
Fouqué, P., Bottinelli, L., Durand, N., Gouguenheim, L., & Paturel, G. 1990, A&AS, 86, 473
Fuentes-Williams, T., & Stocke, J. T. 1988, AJ, 96, 1235
Giovanelli, R., Haynes, M. P., & Chincarini, G. L. 1986, ApJ, 300, 77
Gisler, G. R. 1976, A&A, 51, 137
Giuricin, G., Mardirossian, F., Mezzetti, M., & Monaco, P. 1993, ApJ, 407, 22

Haynes, M. P., & Giovanelli, R. 1984, AJ, 89, 758
———. 1986, ApJ, 306, 466
Helou, G. 1986, ApJ, 311, L33
Huchtmeier, W. K., & Richter, O.-G. 1989a, A&A, 210, 1
———. 1989b, A General Catalog of HI Observations of Galaxies (New York: Springer)
Kennicutt, R. C., Keel, W. C., van der Hulst, J. M., Hummel, E., & Roettiger, K. A. 1987, AJ, 93, 1011
Kennicutt, R. C., & Kent, S. M. 1983, AJ, 88, 1094
Lauberts, A. 1982, The ESO/Uppsala Survey of the ESO(B) Atlas (Munich: European Southern Observatory)
Lauberts, A., & Valentijn, E. A. 1989, The Surface Photometry Catalogue of The ESO-Uppsala Galaxies (Garching-bei-München: European Southern Observatory)
Lonsdale, C. J., Helou, G., Good, J. C., & Rice, W. L. 1985, Cataloged Galaxies and Quasars Observed in the IRAS Survey (Pasadena: Jet Propulsion Laboratory)
MacKenty, J. W. 1989, ApJ, 343, 125
Magri, C., Haynes, M. P., Forman, W., Jones, C., & Giovanelli, R. 1988, ApJ, 333, 136
Maia, M. A. G., & da Costa, L. N. 1990a, ApJ, 349, 47
———. 1990b, ApJ, 352, 457
Maia, M. A. G., da Costa, L. N., & Latham, D. W. 1989 ApJS, 69, 809
Mathewson, D. S., Ford, V. L., & Buchhorn, M. 1992, ApJS, 81, 413
Moss, C., & Whittle, M. 1993, ApJ, 407, L17
Noguchi, M. 1987, MNRAS, 228, 635
Pastoriza, M. G., Bica, E., Maia, M. A. G., Bonato, C., & Dottori, H. 1993, ApJ, submitted
Postman, M., & Geller, M. J. 1984, ApJ, 281, 95
Rowan-Robinson, M., & Crawford, J. 1989, MNRAS, 238, 523
Scodeggio, M., & Gavazzi, G. 1993, ApJ, 409, 110
Thuan, T. X., & Sauvage, M. 1992, A&A, 92, 749
Véron-Cetty, M.-P., & Véron, P. 1991, A Catalogue of Quasars and Active Nuclei (5th ed., Garching-bei-München: European Southern Observatory)
Whitmore, B. C., Gilmore, D. M., & Jones, C. 1993, ApJ, 407, 489